

# Understanding the variable fluorescence quantum yield of tryptophan in proteins using QM-MM simulations. Quenching by charge transfer to the peptide backbone

Patrik R. Callis<sup>\*</sup>, James T. Vivian<sup>1</sup>

*Department of Chemistry and Biochemistry, Montana State University, Bozeman, MT 59717, USA*

Received 17 June 2002; in final form 13 November 2002

## Abstract

A reasonable basis for the puzzling variation of tryptophan (Trp) fluorescence quantum yields in proteins arises naturally through quantum mechanics-molecular dynamics simulations in which the energy of the lowest Trp ring-to-amide backbone charge transfer (CT) state is monitored during dynamics trajectories for 16 Trps in 13 proteins. The energy, fluctuations, and relaxation of the high lying CT state are **highly sensitive to protein environment (local electric field) and rotamer conformation**, leading to large variations in <sup>1</sup>L<sub>a</sub> fluorescence yield and lifetime.

© 2003 Elsevier Science B.V. All rights reserved.

## 1. Introduction

One of the most puzzling phenomena known in applications of fluorescence spectroscopy to proteins is the wide variation of tryptophan (Trp) fluorescence quantum yields ( $\Phi_f$ ) and lifetimes in different protein environments. The yields vary from 0.35 down to 0.01 or less [1]. This is particularly interesting because the light-absorbing part of Trp, effectively 3-methylindole (3MI), shows scant variability in  $\Phi_f$  when dissolved in different solvents varying in polarity from pure hydrocar-

bon to water, being always near 0.3 [2]. The strong sensitivity of Trp fluorescence intensity to protein microenvironment is routinely exploited to follow a variety of protein changes, e.g., ligand/substrate binding, folding/unfolding, etc. [1,3,4]. Although there has been considerable interest in understanding this sensitivity, no convincing detailed mechanism has emerged.

Most pertinent to this Letter is the universal loss of fluorescence quantum yield found for analogues of Trp containing an amide group closely connected to the indole ring by a short aliphatic chain [5,6]. *N*-Acetyltryptophanamide (NATA, see Fig. 1), whose only potential quenching mechanism would appear to be involve an amide group, serves as an icon in this respect:  $\Phi_f$  for NATA in water is 0.14 compared to 0.34 for 3MI [6]. The fluorescence lifetimes of both are single exponen-

<sup>\*</sup> Corresponding author. Fax: +406-994-5407.

E-mail address: [pcallis@montana.edu](mailto:pcallis@montana.edu) (P.R. Callis).

<sup>1</sup> Present address: Golden Helix, 716 S. 20th Ave. Suite 102 Bozeman, MT 59718, USA.

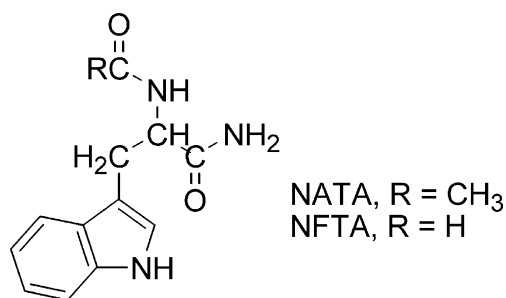


Fig. 1. Structure of *N*-acetyltryptophanamide (NATA, R = CH<sub>3</sub>) and *N*-formyltryptophanamide (NFTA, R = H). All quantum calculations (INDO/S2-SCI) were done on the latter, with geometry and electrical potentials determined from the Charmm 22 forcefield.

tial with NATA showing about a 3-fold reduction in lifetime compared to 3MI [6,7].

The most often proposed mechanism for this loss of  $\Phi_f$  has been electron transfer [7–12]. In particular, the Barkley group has made extensive investigations into the quenching of 3MI by acylated amino acids in solution and concluded that electron transfer quenching by amides in aqueous solution is indeed possible, provided that two or more amide groups are in close proximity. A number of recent works have invoked electron transfer quenching by the local peptide carbonyl group in their explanation of fluorescence lifetime data [13–16].

In this Letter we find that although quantum mechanical calculations place the CT state energy high above (typically 16,000 cm<sup>-1</sup> or 2 eV) the emitting <sup>1</sup>L<sub>a</sub> state in vacuum, they also reveal an extraordinary sensitivity to solvent (local electric field) by the CT state, a property that appears to explain much of the dependence of quantum yield on protein environment in the context of electron transfer theory.

## 2. Methods

We use a generalization of our hybrid QM-MM method used recently to predict fluorescence wavelengths of Trp in proteins [17], wherein the QM part is Zerner's INDO/S-CIS method [18], as modified to include the local electric field and

potentials, and the MM part is Charmm [19]. The main difference is that the QM part is no longer restricted to the indole ring plus C $\beta$  of Trp, but now includes the Trp amide and that of the preceding residue. These are capped with hydrogens so that the QM part is *N*-formyltryptophanamide (Fig. 1).

Other significant expansions of the method are that the geometry for the QM molecule is dictated by the MM (Charmm), allowing the discovery of critical geometries that may stabilize the CT complex. An exception is that in this work we hold the bond lengths constant, using those of the CT state as determined from a CIS/3-21g geometry optimization. The method is further extended to deal with pairs of amino acid residues, wherein one member is the aforementioned *N*-formyltryptophanamide, and the other is the *N*-formyl amide of any other chosen residue of the protein. The pair is then treated as a single molecule (supermolecule).

Among the excited singlet states of the pair are charge transfer (CT) states that may be described as excitation of an electron from a donor molecular orbital (MO) to an empty MO on the acceptor creating a 'radical ion pair'. We note that the supermolecule approach automatically includes the crucially important Coulombic interaction of the radical pair, and relaxations about these charges. The former has been left out of several analyses in the literature. A particularly critical modification of the INDO/S was adoption of a more appropriate set of parameters for oxygen. We have used the values suggested by Li et al. [20].

## 3. Results

Because activationless long range electron transfer quenching of Trp fluorescence by transition metal ions has been demonstrated [21,22], we were open minded about how far and which direction the electron is transferred. However, we found that the lowest CT state almost always involved a local electron transfer from the highest occupied molecular orbital (HOMO), localized on the Trp ring, to the nearest unoccupied backbone amide  $\pi^*$  MO. This is because of the strong Coulombic interaction of the radical pair. For

## increase in charge separation?

example, increasing charge separation by only 1 Å from 5 to 6 Å raises the CT state energy by about 0.5 eV (11 kcal/mol), drastically reducing the probability for transfer. For this reason, we confined the initial investigation to the CT states only, obtaining results that capture the general behavior of the Trp  $\Phi_f$  for the set of 13 proteins selected for study.

Figs. 2 and 3 display the ground  $\rightarrow$  CT and  $^1L_a$  vertical transition energies at the CT geometry during dynamics trajectories for two Trps representing extremes in fluorescence quantum yield: Trp 140 of *Staphylococcus* nuclease (1stn) and Trp 126 of DsbA (1dsbW126) [14]. During the first 50 ps, the Trp charge distribution is that of  $^1L_a$  and during the last 10 ps it is that for the CT state. First, note the enormous energy fluctuations for the CT state, a reflection of its extreme environmental sensitivity. Second, note the large difference in CT- $^1L_a$  energy gap for the two cases. For 1stn, the probability that the CT and  $^1L_a$  states will cross during the excited state lifetime because of a large downward fluctuation is insignificant, a result that correlates with the high quantum yield

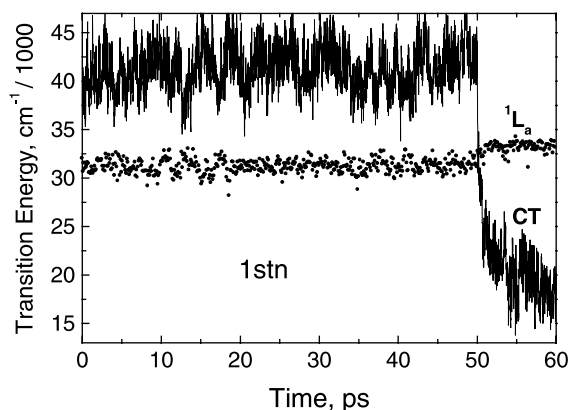


Fig. 2. Vertical transition energy,  $\Delta E/1000$  hc for the ground  $\rightarrow$   $^1L_a$  state (dots) and the ground  $\rightarrow$  lowest Trp ring-amide charge transfer (CT) state transitions (line) both at the CT state geometry during a 60 ps QM-MM trajectory for Trp 140 of *Staph.* nuclease (1stn), solvated by a 25 Å radius sphere of explicit water. During the first 50 ps the charges on the Trp are those of the  $^1L_a$  state (scaled by 0.80) and are updated every 10 fs. During the last 10 ps the charges are those of the CT state. Note the much greater fluctuation amplitude for the CT state than for  $^1L_a$ . This protein has a high Trp fluorescence quantum yield.

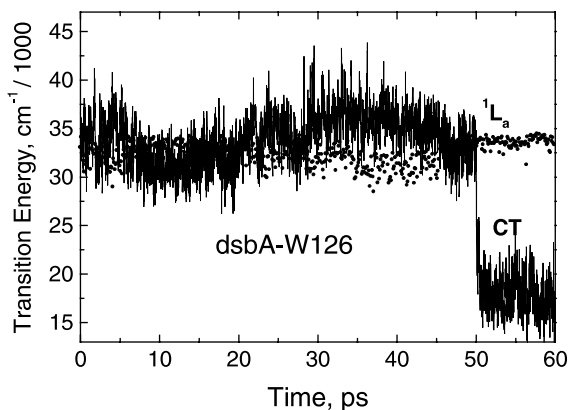


Fig. 3. Same as Fig. 2 except for 1dsb-W126. Note the much lower energy and faster relaxation of the CT state, which correlates with the low quantum yield (0.01) found for 1dsbW126 [14].

observed for this case, 0.3. In contrast, the CT- $^1L_a$  gap for 1dsbW126 is close to zero during most of the trajectory, and there are many crossings during the excited state lifetime.

The origin of the large difference in gap for these and other cases can be traced to the local electric field (potential difference) caused not only by the intermolecular electrostatic interactions, but also by intramolecular differences in the coulombic energy of the separated charges for different rotameric conformations. A more detailed description is planned for a future publication. Next we turn attention to what happens after an electron transfer event.

During the last 10 ps of the trajectories, the charges on the Trp are always those of the CT state, as determined from the QM for the previous point in time. That is, a simulated electron transfer was executed. What is seen in both cases (but especially for 1dsbW126), is an initially very fast, and ultimately large relaxation of the CT energy primarily due to solvent reorientation. The formation of the solvent stabilized charge separated state, a specific assignment to the generic dark state (small radiative rate) proposed by Hudson et al. [11] with energy well below that of  $^1L_a$ , is also a requirement for quenching; otherwise the system would quickly return to the fluorescent state.

Fig. 4 shows the CT (top) and  $^1L_a$  (middle) average transition energies, with their standard deviations indicated, and the solvent relaxed CT

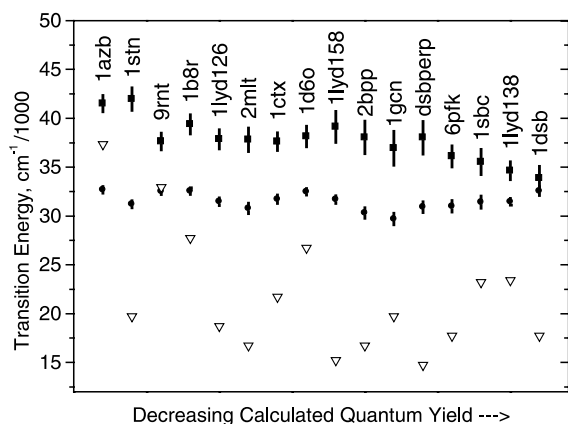


Fig. 4. Condensation of data from QM-MM trajectories for 16 Trps from 13 proteins in order of decreasing Trp fluorescence quantum yield as calculated from Eq. (3). Solid squares, average CT energy with standard deviation given by twice the vertical line; Solid circles, average  $^1L_a$  energy with standard deviation given by twice the vertical line; open inverted triangles, average energy of the relaxed CT state, from the last 5 ps of the trajectory. The labels refer to Protein Data Bank X-ray structure codes.

transition energy (inverted triangles) for the full set of 16 Trps in 13 proteins studied. The points are arrayed in order of decreasing calculated  $\Phi_f$ , with the highest yield on the left.

Although not the main thrust of this communication, it is interesting to make some correlations that indicate a promising path to quantitative prediction. The primary message of this Letter is that the smaller the CT- $^1L_a$  gap and larger the fluctuations, the higher is the probability of the  $^1L_a$ -CT transition. A common approximation is that the electron transfer rate constant,  $k_{ET}$ , should correlate with the magnitude of the normalized Gaussian probability distribution of the  $^1L_a$ -CT energy difference corresponding to zero difference,  $P(0)$  [23,24]. This is given in terms of the mean gap value between  $^1L_a$  and CT states with both at equilibrium internal geometry,  $\langle\Delta E_0\rangle$  and its standard deviation,  $\sigma$ , as

$$P(0) = (2\pi\sigma^2)^{-1/2} \exp\left(-\frac{1}{2}\left(\frac{\langle\Delta E_0\rangle}{\sigma}\right)^2\right). \quad (1)$$

This form maps onto the well known equation [25,26],

$$k_{ET} = \left(\frac{4\pi^2}{h}\right) V^2 F (4\pi\lambda k_B T)^{-1/2} \times \exp\left(-\frac{(\Delta G_0 + \lambda)^2}{4\lambda k_B T}\right), \quad (2)$$

where  $h$  = Planck's constant,  $V$  = the electronic coupling matrix element between the  $^1L_a$  and CT states,  $F$  is the Franck-Condon factor governing the internal high frequency vibrational mode reorganization,  $\lambda$  is the solvent and low frequency solute vibrational reorganization energy,  $k_B$  = Boltzmann constant,  $\Delta G_0$  = the difference in free energy of the equilibrium states. The mapping is therefore:  $\langle\Delta E_0\rangle = \Delta G_0 + \lambda$  and  $\sigma^2 = 2\lambda k_B T$ . In terms of  $\langle\Delta E_0\rangle$  and  $\sigma$ , and using  $\text{cm}^{-1}$  as the energy unit, Eq. (2) becomes:

$$k_{ET} = \frac{4\pi^2 c}{\sqrt{4\pi}} \frac{V^2 F}{\sigma} \exp\left(-\frac{1}{2}\left(\frac{\langle\Delta E_0\rangle}{\sigma}\right)^2\right), \quad (3)$$

where  $4\pi^2 c / (4\pi)^{1/2} = 4.724 \times 10^{11} \text{ cm/s}$ , and  $c$  = the velocity of light.

The fluorescence quantum yield,  $\Phi_f$ , is given by

$$\Phi_f = k_r / (k_r + k_{nr} + k_{et}),$$

where  $k_r$  and  $k_{nr}$  are the radiative and the non-electron transfer non-radiative rate constants. Here we use  $k_r = 4 \times 10^7 \text{ s}^{-1}$  and  $k_{nr} = 9 \times 10^7 \text{ s}^{-1}$  [7]. We do not now try to estimate  $V^2 F$ , and we estimate  $\langle\Delta E_0\rangle$  by adding a reasonable energy to the vertical value found with the CT state geometry,  $\langle\Delta E_{\text{vert}}\rangle$  (as seen in Figs. 2 and 3) We adjust  $V^2 F$  to get a reasonable global fit with experiment, assuming that  $V$  is the same for all cases. Our view is that  $V$  is *not* the rate limiting factor and that, in any event, one cannot assume an exponential distance dependence for  $|V^2|$  at such close range [27,28].

Fig. 5 shows a plot of predicted  $\Phi_f$  values as a function of observed  $\Phi_f$  for which  $\langle\Delta E_0\rangle = \langle\Delta E_{\text{vert}}\rangle + 700 \text{ cm}^{-1}$  and  $k_{ET}$  is found from Eq. (3) using  $V = 120 \text{ cm}^{-1}$  and  $F = 0.01$ , numbers that are not unreasonable. Despite the approximation of assuming constant  $V$ , the fit captures the known variability of  $\Phi_f$  in a way that generally agrees with experiment, with a few egregious disagreements. The fit is not very sensitive to the choice of parameters.

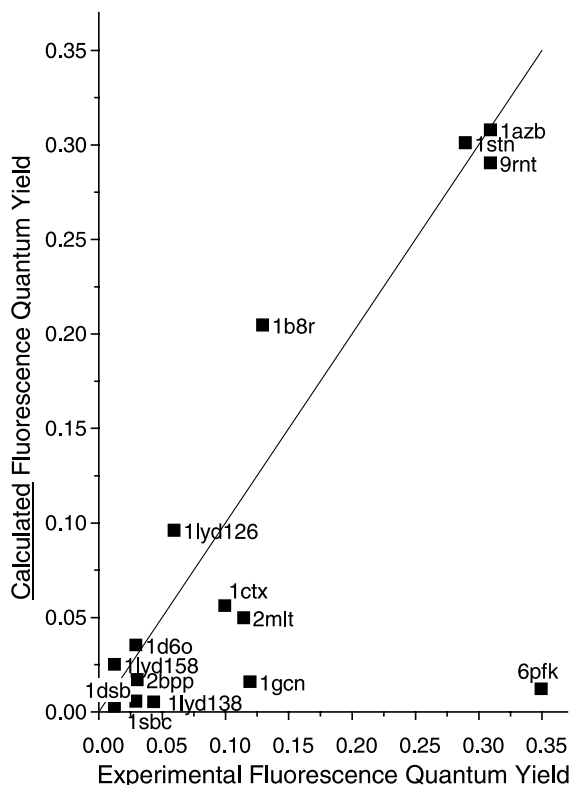


Fig. 5. Plot of Trp fluorescence quantum yields calculated using Eq. (3) (except for 9rnt) as a function of observed quantum yields for the set of Trps in Fig. 4. The yield for 9rnt (ribonuclease T1) did not use Eq. (3) because the scaled energy of the relaxed CT state was above the  $^1L_a$  state. The Boltzmann factor was used instead. The line represents perfect agreement. A linear regression through zero for all points gives a correlation coefficient = 0.7, which improves to 0.93 if pfk is left out. Observed quantum yields were from [1], except for the following: 1dsbW126 [14]; for 1d6o the quantum yield is an upper limit based on the 12-fold increase upon denaturation [D.A. Egan et al., *Biochemistry* 32 (1993) 1920]; 1ld [D.L. Harris, B.S. Hudson, *Chem. Phys.* 158 (1991) 353]. The value for 1sbc (subtilisin Carlsberg) was estimated from the lifetimes given in [1].

#### 4. Discussion

We have benefited from numerous QM-MM applications to electron transfer, for example [29–31], but this seems to be the first specific application to the Trp – amide system. The main purpose of this communication is to articulate a promising new and more detailed view of Trp quenching. The idea is that local electric potential differences and

solvent mobility are crucial in determining whether a particular group will be an effective electron acceptor or not. Thus, *the location of charged groups along the line connecting the Trp ring and electron acceptor will strongly influence the rate of electron transfer*. For example, an aspartate group (or any negatively charged group) near the benzene ring end of Trp and farther from the amide will lower the energy of the CT state, and contribute to lowering the quantum yield. Replacing such a group with a neutral residue would likely increase the yield, giving the erroneous impression that aspartate was the electron acceptor. Were the aspartate on the opposite side, near the amide, the opposite result would be expected. The anomalous pH dependence of Trp 138 quenching by histidine in T4 lysozyme [32] can be explained in terms of this electrostatic mechanism.

Notice that the main principle here is independent of the exact nature of the CT state, leaving the possibility for  $\pi\sigma^*$  type states that have recently come to light from high level quantum chemical computations [33].

Presently there are many candidates for the few egregious failures of prediction in Fig. 5, including the assumption of linear response (known to be suspect [34]), use of one  $V$  for all, uncertainties in X-ray structures (e.g., rotamer states), protonation states, energy of the CT state, criterion for identifying the lowest CT state (how much charge needs to be transferred before we call the state a CT state), the charge model (how much we scale the QM charges and the validity of the force field assigned point charges), electronic polarizability, solvation details, and the extent of intermolecular quenching. Most of these potentially affect  $\sigma$  and  $\langle\Delta E_0\rangle$ , upon which the predictions are very sensitive. For example, 1b8r (cod parvalbumin) is corrected by a decrease in gap of only  $500\text{ cm}^{-1}$  (0.063 eV) or an increase in  $\sigma$  of only  $200\text{ cm}^{-1}$ . We are actively working on improving the method.

#### 5. Conclusion

Trp fluorescence quantum yield and lifetime dependence on protein environment arise mainly from the average local electric potential difference

between the Trp ring and local backbone amide and from the amplitude of the variability of this potential difference caused by protein and solvent motions. Quenching occurs by internal conversion to the very weakly emitting charge transfer (CT) state when fluctuations reduce the CT-<sup>1</sup>L<sub>a</sub> energy gap to zero followed by fast solvent relaxation about the CT state to create a low-lying solvent stabilized ‘radical ion pair’. Non-exponential fluorescence decay may be expected to arise naturally through various mechanisms in this view.

### Acknowledgements

This work was supported by NSF grants MCB-9817372 and MCB-0133064. We also appreciate encouraging conversations with Drs. Frank Prendergast, Bruce Hudson, and Mary Barkley. We thank Dr. Tiqing Liu for helping run the simulations.

### References

- [1] M.R. Eftink, *Methods Biochem. Anal.* 35 (1991) 127.
- [2] S.R. Meech, A. Lee, D. Phillips, *Chem. Phys.* 80 (1983) 317.
- [3] A.P. Demchenko, *Ultraviolet Spectroscopy of Proteins*, Springer, New York, 1986.
- [4] J. Ervin, J. Sabelko, M. Gruebele, *J. Photochem. Photobiol. B* 54 (2000) 1.
- [5] W.J. Colucci, L. Tilstra, M.C. Sattler, F.R. Fronczek, M.D. Barkley, *J. Am. Chem. Soc.* 112 (1990) 9182.
- [6] M.R. Eftink, Y. Jia, D. Hu, C.A. Ghiron, *J. Phys. Chem.* 99 (1995) 5713.
- [7] Y. Chen, M.D. Barkley, *Biochemistry* 37 (1998) 9976.
- [8] R.F. Steiner, E.P. Kirby, *J. Phys. Chem.* 73 (1969) 4130.
- [9] P.M. Froehlich, K. Nelson, *J. Phys. Chem.* 82 (1978) 2401.
- [10] Y. Chen, B. Liu, H.-T. Yu, M.D. Barkley, *J. Am. Chem. Soc.* 118 (1996) 9271.
- [11] B.S. Hudson, J.M. Huston, G. Soto-Campos, *J. Phys. Chem. A* 103 (1999) 2227.
- [12] Z. Bajzer, F.G. Prendergast, *Biophys. J.* 65 (1993) 2313.
- [13] A. Ababou, E. Bombarda, *Protein Sci.* 10 (2001) 2102.
- [14] A. Sillen, J. Hennecke, D. Roethlisberger, R. Glockshuber, Y. Engelborghs, *Proteins Struct. Funct. Genet.* 37 (1999) 253.
- [15] A. Sillen, J.F. Diaz, Y. Engelborghs, *Protein-Sci.* 9 (2000) 158.
- [16] P.D. Adams, Y. Chen, K. Ma, M.G. Zagorski, F.D. Sonnichsen, M.L. McLaughlin, M.D. Barkley, *J. Am. Chem. Soc.* 124 (2002) 9278.
- [17] J.T. Vivian, P.R. Callis, *Biophys. J.* 80 (2001) 2093.
- [18] J. Ridley, M. Zerner, *Theor. Chim. Acta (Berl.)* 32 (1973) 111.
- [19] A.D. MacKerell Jr., D. Bashford, M. Bellott, R.L. Dunbrack, J.D. Evanseck, M.J. Field, S. Fischer, J. Gao, S. Ha, D. Joseph-McCarthy, L. Kuchnir, K. Kuczera, F.T.K. Lau, C. Mattos, S. Michnick, T. Ngo, D.T. Nguyen, B. Prodhom, W.E. Reiher III, B. Roux, M. Schlenkrich, J.C. Smith, R. Stote, J. Straub, M. Watanabe, J. Wiorkiewicz-Kuczera, D. Yin, M. Karplus, *J. Phys. Chem. B* 102 (1998) 3586.
- [20] J. Li, B. Williams, C.J. Cramer, D.G. Truhlar, *J. Phys. Chem.* 110 (1999) 724.
- [21] J.W. Petrich, J.W. Longworth, G.R. Fleming, *Biochemistry* 26 (1987) 2711.
- [22] R.M. Supkowski, J.P. Bolender, W.D. Smith, L.E.L. Reynolds, W.D. Horrocks, *Coord. Chem. Rev.* 185 (1999) 307.
- [23] J.J. Hopfield, *Proc. Natl. Acad. Sci. USA* 71 (1974) 3640.
- [24] N.R. Kestner, J. Logan, J. Jortner, *J. Phys. Chem.* 78 (1974) 2148.
- [25] M. Bixon, J. Jortner, *Adv. Chem. Phys.* 106 (1999) 35.
- [26] R.A. Marcus, N. Sutin, *Biochim. Biophys. Acta* 811 (1985) 265.
- [27] D.N. Beratan, J.N. Betts, J.N. Onuchic, *J. Phys. Chem.* 96 (1992) 2852.
- [28] I.V. Kurnikov, D.N. Beratan, *J. Chem. Phys.* 105 (1996) 9561.
- [29] A. Warshel, *J. Phys. Chem.* 86 (1982) 2218.
- [30] E. Carter, J.T. Hynes, *J. Chem. Phys.* 94 (1991) 5961.
- [31] J.N. Gehlen, M. Marchi, D. Chandler, *Science* 263 (1994) 499.
- [32] M. Van Gilst, B.S. Hudson, *Biophys. Chem.* 63 (1996) 17.
- [33] A.L. Sobolewski, W. Domcke, C. Dedonder-Lardeux, C. Jouvet, *Phys. Chem. Chem. Phys.* 2002 (2002) 1093.
- [34] G. King, A. Warshel, *J. Chem. Phys.* 93 (1990) 8682.